Agricultural and Forest Meteorology 213 (2015) 203–216

Contents lists available at ScienceDirect

Agricultural and Forest Meteorology

journal homepage: www.elsevier.com/locate/agrformet

Empirical stomatal conductance models reveal that the isohydric behavior of an *Acacia caven* Mediterranean Savannah scales from leaf to ecosystem

Nicolas Raab[a,*,1], Francisco Javier Meza[b,c], Nicolás Franck[d], Nicolás Bambach[e]

[a] Departamento de Fruticultura y Enología, Facultad de Agronomía e Ingeniería Forestal, Pontificia Universidad Católica de Chile, Av. Vicuña Mackenna 4860, 7820436 Macul, Santiago, Chile
[b] Departamento de Ecosistemas y Medio Ambiente, Facultad de Agronomía e Ingeniería Forestal, Pontificia Universidad Católica de Chile, Av. Vicuña Mackenna 4860, 7820436 Macul, Santiago, Chile
[c] Centro Interdisciplinario de Cambio Global, Pontificia Universidad Católica de Chile, Av. Vicuña Mackenna 4860, 7820436 Macul, Santiago, Chile
[d] Centro de Estudio de Zonas Aridas & Departamento de Producción Agrícola, Facultad de Ciencias Agronómicas, Universidad de Chile, Casilla 129, 1780000 Coquimbo, Chile
[e] Department of Land, Air and Water Resources, University of California, Davis, One Shields Avenue, CA 95616, USA

ARTICLE INFO

Article history:
Received 19 August 2014
Received in revised form 12 June 2015
Accepted 24 June 2015
Available online 25 July 2015

Keywords:
Canopy conductance
Mediterranean Savannah
Drought
Empirical models
Acacia caven

ABSTRACT

Canopy conductance (g_c) is the main controller of plant-atmospheric interaction and a key element in understanding how plants cope with drought. Empirical g_c models provide a good inference as to how environmental forcing affects surface water vapor and CO_2 gas exchange. However, when facing water scarcity, soil moisture or plant water availability becomes the primary controller. We studied g_c in an *Acacia caven* (Mol) savannah in Central Chile under Mediterranean-type climate conditions that present distinguishable wet and dry seasons. We calibrated an empirical g_c, in order to account for whole canopy gas exchange with g_c measurements from three different data sets: (1) an inversion of the Penman–Monteith equation in combination with a Shuttleworth and Wallace model (PMSW) for evapotranspiration from sparse canopies; (2) an inversion of the Penman–Monteith (PM) based on the big leaf approach and (3) a set of leaf stomatal conductance (g_s) ground based measurements taken throughout the season and scaled up to the canopy level. Then the semi-empirical Farquhar–Ball–Berry (FBB) g_c model was added to the comparison to evaluate if the inclusion of a mechanistic component for photosynthesis would improve the prediction of g_c. Models performance was assessed with ground based leaf gas exchange measurements during both wet and dry seasons. *Acacia's* g_c showed a high synchronicity with soil moisture, exhibiting the typical isohydric behavior of this kind of vegetation. The addition of the Shuttleworth and Wallace modifier to the Penman–Monteith equation did not yield a better calibration for the multiplicative model when compared to the one calibrated with the PM g_c data set, however this does not directly certifies that PM itself is a better estimator of g_c in sparse canopies. Furthermore, scaling issues such as ecosystem heterogeneity and patchiness must be considered when applying these estimations to a watershed level for both eco and hydrological reasons. These empirical models demonstrated to be a good tool for predicting stomatal behavior for this kind of vegetation. Nevertheless, the effect of deep soil moisture on plant water status must be integrated in g_c estimations in order to improve model's performance.

© 2015 Elsevier B.V. All rights reserved.

1. Introduction

Mediterranean ecosystems represent only around 2 percent of the Earth's surface, yet they play a key role as biodiversity reserves being shelters of about 20 percent of the planet's flora, most of which is highly endemic (Cowling et al., 1998). These ecosystems are in compass with a climate characterized by a strong seasonality. Precipitation and temperature are dichotomous, with tempera-

* Corresponding author.
E-mail address: nraab@uc.cl (N. Raab).
[1] Present address: Environmental Change Institute, School of Geography and the Environment, University of Oxford, South Parks OX1 3QY, Oxford, UK.

http://dx.doi.org/10.1016/j.agrformet.2015.06.018
0168-1923/© 2015 Elsevier B.V. All rights reserved.

ture trends reaching maxima during the summer months and precipitation reaching maxima during winter months. Soil water availability plays a major limiting role in vegetation growth, and secular regional changes in temperatures and precipitation are believed to be already inducing changes in this type of ecosystems (Keenan et al., 2009). Climate models predict further increases in temperature in the future, with changes in rainfall patterns. Furthermore, despite the fact that net ecosystem exchange from arid and semi-arid ecosystem is regarded as low, these ecosystems represent between 42 and 56% of the world's land (Melillo et al., 1993), hence their importance in both global carbon and water balance. Central Chile represents one of the five regions of the world with a Mediterranean-type climate, where drought is a dominant feature. The region is characterized by a long dry season with the complete absence of rainfall from mid spring to mid fall. Vegetation consists mainly of sclerophyllous shrubs, where *Acacia caven* (Mol) is a dominant species. From Africa to Australia the *Acacia* genus has shown a wide range of adaptations to water scarcity (Cleverly et al., 2013; Eamus et al., 2013; Grouzis et al., 1998; Pohlman et al., 2005; Otieno et al., 2005;) allowing it to cope with severe droughts. Therefore *A. caven* can be considered as an archetype plant for understanding a plant canopy behavior when facing drought and to test model performance under scenarios of water scarcity.

Stomatal conductance (g_s) is the main path through which plants control both leaf transpiration and CO_2 intake (e.g.: Reichstein et al., 2002; Krishnan et al., 2006; Kljun et al., 2007; Keenan et al., 2009), and one of the main mechanisms through which plants cope with drought stress (Damour et al., 2010). Farquhar et al. (1980) represented leaf photosynthesis as a process dominated by light and internal CO_2 concentration (C_i), which in turn depends on g_s and net assimilation rate (A_n). Leaf stomatal conductance and photosynthesis can be scaled-up to canopy level by considering several assumptions attempting to represent complex heterogeneities ubiquitously found in plant canopies. Canopy conductance is the main lock of the soil–plant–atmosphere water continuum, driving both nutrient uptake and soil water depletion (Berry et al., 2010; Damour et al., 2010), thus it is considered a key and complex variable in most land-surface models (Medlyn et al., 2011).

Mechanistic and empirical model approaches have been used to represent g_c. Mechanistic models rely upon g_c response to internal physiological processes that drive stomatal behavior, whereas empirical models have simplified the representation of g_c by relating observed canopy responses to changes in environmental conditions based on a purely statistical parameterization without any specific physiological meaning. Multiplicative models based on an empirical approach establish a set of penalty functions modifying a maximal g_c while accounting for environmental covariates (Jarvis, 1976). On the other hand, semi-empirical models are based on g_s behavior but can be later scaled up to the canopy level, aiming to mix both mechanistic and empirical approaches. After Wong et al. (1979) showed that stomatal movement not only responds to plant water status but also on leaf A_n, Ball et al. (1987) aimed to couple g_s to A_n through Farquhar et al. (1980) mechanistic model for leaf carbon exchange and performing a statistical fitting between A_n and g_s, which resulted in the Farquhar–Ball–Berry (FBB) semi-empirical model (Dewar, 2002).

Empirical models have been largely used at the field level (e.g.: Stewart, 1988; Grace et al., 1995; Van Wijk et al., 2000; Harris et al., 2004). However, when facing drought conditions, it is necessary to introduce some modifications. Models based on photosynthesis depend on a linear relationship between g_s and A_n that could change depending on plant water status (Tenhunen et al., 1990). Empirical multiplicative models can add the effect of soil water availability or plant water status as another environmental factor regulating g_c. Similar water status restrictions can be applied in semi-empirical models, thus accounting for isohydric behavior (Tardieu and Simonneau, 1998). However, since empirical approaches have been developed under a constrained range of environmental variables, extreme conditions such as high vapor pressure deficit, low water availability or extreme temperatures, challenge the ability of these models to accurately estimate g_c (Gao et al., 2002).

We aim to use a combination of observational and modeling techniques in order to account for the effect of drought stress on gas exchange. Accordingly, we first evaluate different methodologies to obtain *Acacia's* g_c linking latent heat (λE) to canopy's resistance to water loss. We assessed the inversion of the Penman–Monteith (PM) equation based on the big leaf approach, thus obtaining hourly g_c measurements. Furthermore, in order to consider the nature of a sparse canopy such as the Savannah in this study, a combination of PM with the Shuttleworth and Wallace (PMSW) was evaluated. Ecosystem λE was obtained from Eddy Covariance measurements for both the PM and PMSW approaches. Secondly, both g_c measurements were used to calibrate a multiplicative model integrating soil moisture as an environmental covariate, additionally, a third calibration was performed with ground-based measurements of g_s, scaled up to canopy level (g_c). Finally, a semi-empirical model based on the FBB approach was added to the comparison in order to evaluate how a mechanistic approach could improve g_c estimations. All models outputs were compared against ground-based measurements in order to evaluate their performance in the field. By comparing g_c models which use different approaches and have different calibrations, we aim to select the best model that allows us to (a) have a good estimate of water and CO_2 fluxes through g_c behavior and (b) help us understand how plants' strategy for regulating water loss (i.e. iso or anisohydric behavior) influences the seasonality of Mediterranean ecosystem fluxes.

2. Materials and methods

2.1. Site and data description

The study site corresponds to a 24Ha shrubland Savannah in Central Chile (33°02′S, 70°44′W), located at 660 m above the sea level with an average slope of less than 5%. The climate can be regarded as Mediterranean, with a mean annual temperature of 15.6 °C and a total mean annual precipitation of 245 mm. The site is characterized by wet and dry seasons when the majority of rainfall is concentrated between May and September, and a long dry summer extending from October to April. This type of climate shows particularly high values of water vapor deficit during spring and summer, as relative humidity is usually below 50% and daily temperatures exceed 30 °C.

The Savannah is dominated by *A. caven* trees sparsely distributed throughout the field. The soil corresponds to a Mollisol with a bulk density of 1.4 g cm^{-3} and a clay–loam texture. During late winter and early spring a herbaceous layer mainly consisting of *Anoda* sp., *Erodium moschatum*, *Trifolium* sp., *Oxalis* sp., *Urtica hurens* and *Helenium aromanticum* is observed, however during the dry season the field is completely dominated by *A. caven*. *Acacia* trees on the study site show clear signs of re-sprouting given the fact that most parts of central Chile's shrublands were logged for charcoal production during the last two centuries. Nevertheless, the field was acquired seven years ago by a third party and has since been used for conservation purposes thus eradicating logging and human fire risks, although the sporadic presence of cattle (herbivory) was observed.

Canopy coverage fraction (f_c) is 0.25. Trees coverage was determined by satellite images obtained from Google Earth during the dry season and later analyzed through a self-made Matlab script (Mathworks, MA, USA). Because *Acacia* crowns in grey scale images

were darker than bare soil, a darkness threshold was established and pixels that were beyond that threshold were aggregated and then divided by the total amount of pixels, more details about this method can be found in Appendix A. The same process was done for six different images; all of them giving values close to 0.25. Mean canopy height was around 3.2 m. During the study period, *Acacia*'s leaf area index (L_0) was 0.7, without any observed large variation over the season. Because of its shrub nature, *Acacia*'s L_0 is difficult to assess through ground based methods due to the high degree of clumping that this kind of vegetation exhibits (Ryu et al., 2010), we estimated the ecosystem's leaf area index (LAI) through normalized difference vegetation index (NDVI) images corresponding to the pixel with the largest fetch, LAI values from NDVI images were computed by the Oak Ridge National Laboratory Distributed Active Archive Center (ORNL DAAC, 2014). *Acacia*'s LAI values were obtained from the dry season to avoid understory contribution to ecosystem LAI. Ecosystem LAI was then corrected by f_c, thus resulting in L_0.

Fig. 1 shows the evolution of daily minimum soil water content, *SWC*, together with ecosystem's LAI, daily *Acacia* transpiration and soil evapotranspiration rates. The Savannah is characterized by a clear seasonality. During the wet season, together with high values of *SWC*, an increase in ecosystem's LAI is observed because of the development of the understory, thus, increasing soil's evapotranspiration rates. However, during the dry season, along with the loss of the herbaceous layer, ecosystem evapotranspiration becomes completely dominated by *Acacia*'s g_c.

Carbon and water vapor flux data were measured with an Eddy Covariance station at a height of 5.2 m with a time averaged step of 30 min. The maximal fetch of the station was registered at 700 m, yet 90% of the fluxes came from 100 m in the upwind direction. The dataset covered from October 2011 (Spring) to January 2013 (Mid Summer), encompassing two dry seasons and one wet season. Water vapor and CO_2 densities were measured at 10 Hz with an infrared gas analyzer (Li 7500, Licor, Lincoln, NE, USA). Wind speed and sensible heat flux were measured with a 3 dimensional anemometer (CSAT3, Campbell, Logan, UT, USA) at the same frequency. Net radiation (R_n) was measured with a net radiometer (NR-LITE, Kipp&Zonen, Delft, Netherlands), at a height of 5 m above ground. Soil heat flux (G) was measured with two soil heat flux plate systems (HFP01, Hukseflux Thermal Sensors, Delf, Netherlands) buried at a depth of 0.1 m. One plate system was installed below an *Acacia* crown while the other was installed under bare soil. Photosynthetically active radiation (*PAR*) was measured with a silicon quantum sensor (LI 190, Licor, Lincoln, NE, USA). Canopy temperature was consider as a proxy for Leaf temperature (T_l), which was used to determine leaf-to-air water vapor deficit (D_l) and was obtained by one infrared thermometer (Apogee SI-190, Logan, UT, USA) pointing to a representative crown sampled at 3 Hz. Soil water content was determined with two time-domain reflectometers (TDR) (CS-616, Campbell Scientific INC, Logan, UT, USA) installed at 0.1 m below the surface, next to each soil heat flux plate pairs. Raw data was stored in a data logger (CR5000, Campbell Scientific INC, Logan, UT, USA). We eliminated flux data 48 h after rain events since ecosystem λE is dominated by canopy evaporation rather than canopy transpiration (Harris et al., 2004). Total available data covered more than 450 days (10,964 h), with an acceptable mean energy balance closure close to 70% during daytime (Wilson et al., 2002; data not shown).

2.2. Linking canopy conductance to latent heat flux

2.2.1. Computing evapotranspiration from sparse canopies

We used the Shuttleworth and Wallace (1985) model for λE transfer from sparse canopies, that relies on a unique mean canopy airstream (Fig. 2) accounting for all ecosystem water vapor sources. As sparse canopies allow for aerodynamic mixing within the surface (Thom, 1972), the result is a single airstream composed of partial contributions from all ecosystem water vapor sources. Accordingly, ecosystem latent heat flux (λE_{eco}) can be represented as (Brenner and Incoll, 1997):

$$\lambda E_{eco} = f_c(\lambda E_c + \lambda E_s) + (1 + f_c)(\lambda E_{bs}) \quad (1.a)$$

$$\lambda E_{eco} = f_c(\lambda E_c + \lambda E_{ML.s}) + (1 - f_c)(\lambda E_{ML.bs}) \quad (1.b)$$

where λE_s and λE_{bs} are latent heat fluxes from the soil and bare soil respectively, while λE_c is canopy latent heat flux, all units are W m^{-2}. Accordingly, $\lambda E_{ML.s}$ and $\lambda E_{ML.bs}$ correspond to the evaporation rates obtained from the micro-lysimeters placed in the soil and bare soil substratum respectively.

2.2.2. Ecosystem latent heat flux partitioning

As Eddy Covariance measurements do not distinguish the individual contribution of each element (canopy, soil and bare soil) to λE_{eco}, estimates of λE_s and λE_{bs} are needed in order to solve for λE_c in Eq. (1.a) Both λE_s and λE_{bs} were calculated as a weight difference from micro-lysimeters adapted from Liu et al. (2002). Micro-lysimeters consisted of plastic collars of 0.11 m diameter and 0.2 m length, enclosed by a perforated bottom cap. We installed six units across the field, without disturbing soil structure, at 100 m in the upwind direction from the Eddy Covariance station, thus representing the area of maximal fetch. Three micro-lysimeters were installed in the soil under *Acacia* trees, representing λE_s conditions, positioned towards North, East and South from the trunk in order to expose them to different energy budgets. The other three micro-lysimeters were installed in the bare soil, representing bare soil evaporation (Fig. 2). During the wet season, bare soil micro-lysimeters developed an herbaceous stratum, similar to understory's natural conditions.

All micro-lysimeters were weighed in the field once a week, and before and after rain events using a scale with a 1 g precision (i.e. equivalent to 0.12 mm). Mean values for each group of micro-lysimeters represented the evaporation from the soil and the bare soil respectively. To get both soil and bare soil instantaneous evapotranspiration, as given by Eddy Covariance measurements, data from micro-lysimeters weight difference was multiplied by the ratio between instantaneous reference evapotranspiration, ET_0 (calculated following Allen et al., 1998), obtained at each 30 min interval, and total ET_0 registered during the week. The equation for the disaggregation procedure is:

$$\lambda E_{ML} = \lambda \sum_1^7 E_{ML} \times \frac{ET_0}{\sum_1^7 ET_0} \quad (2)$$

where λ is the latent heat of vaporization (J kg^{-1}), E_{ML} is the evaporation rate from micro-lysimeters in mm s^{-1}, $\sum_1^7 E_{ML}$ is total weekly evaporation, from day one to seven, obtained from the micro-lysimeters and expressed in mm $week^{-1}$. ET_0 is the instantaneous reference evapotranspiration (mm s^{-1}), whereas $\sum_1^7 ET_0$ is the total reference evapotranspiration over a week (mm $week^{-1}$). The underlying assumption is that soil bulk surface resistance is controlled by the degree of water retention by the soil matric potential, mostly related to soil water content. As soil water content is not expected to show major variations over a week, except after a rain event, r_s^s and r_s^{bs} are assumed constant (Mahrt and Pan, 1984), coupling both soil and bare soil evaporation rates to atmospheric water demand given by ET_0. After replacing the obtained values for both bare soil and soil substratum from averaging the two sets of micro-lysimeters in Eq. (1.b); λE_c is computed since λE_{eco} is given by the Eddy Covariance station.

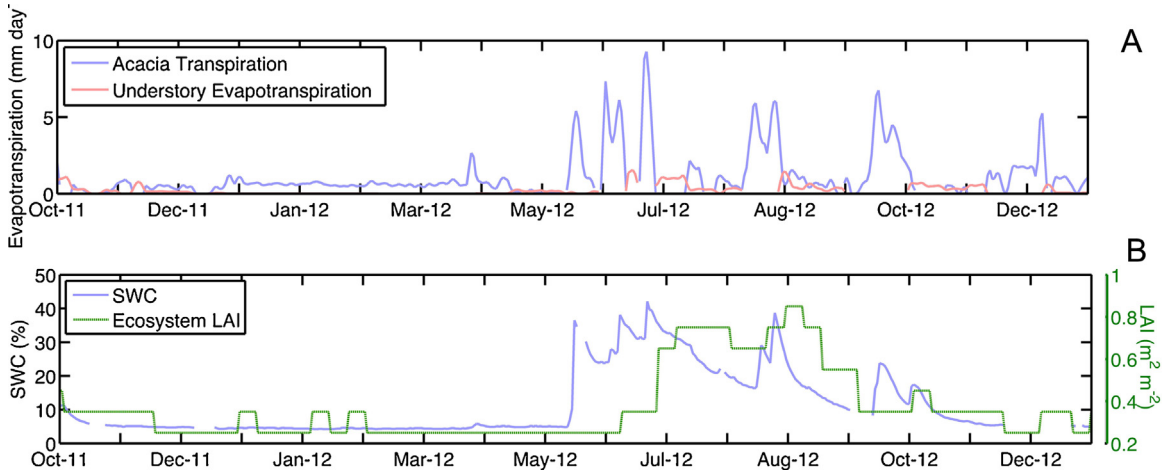

Fig. 1. On (A) Evolution of canopy transpiration and soil evapotranspiration; on (B) daily minimum soil water content (*SWC*) and ecosystem's leaf area index (LAI) daily values throughout the season. Ecosystem dynamics are marked by seasonality between dry (October–April) and wet season (May–September).

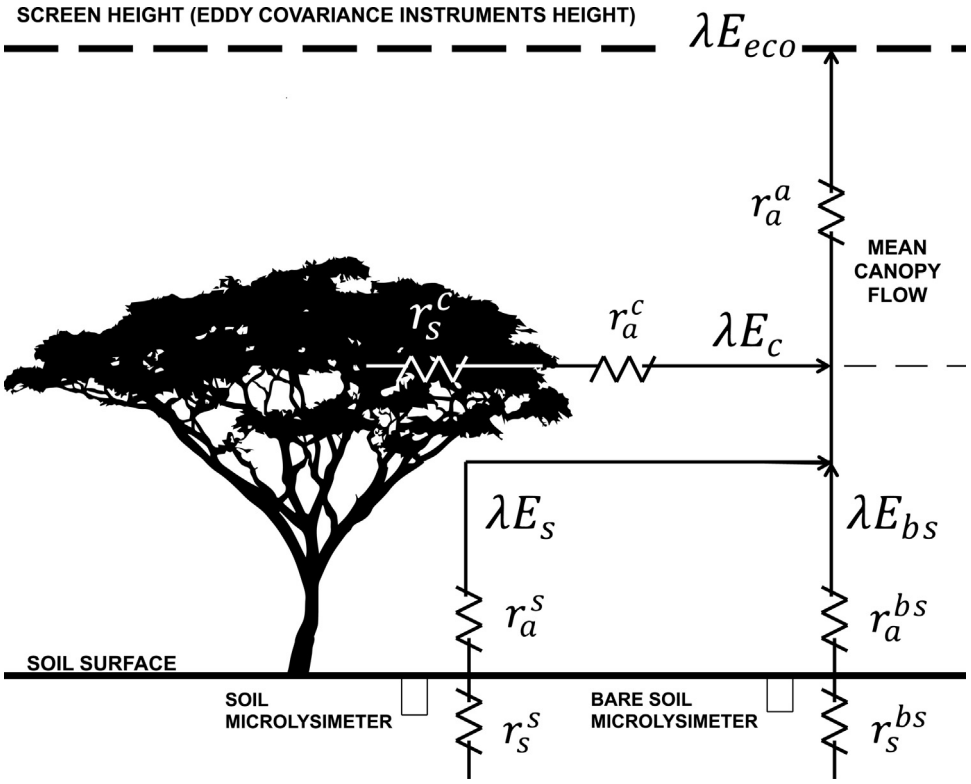

Fig. 2. Diagram of the Ecosystem latent heat flux partitioning from sparse canopies. r_s^c, r_s^s and r_s^{bs} are bulk surface resistance for canopy, soil and bare soil respectively. r_a^c, r_a^s and r_a^{bs} correspond to aerodynamic resistances for each of the elements listed above. Finally, r_a^a is the resistance for turbulent transport from source to screen height. All resistances are expressed in s m^{-1}.

2.2.3. Calculating canopy conductance through canopy latent heat flux

By obtaining λE_c we applied the inverted Penman–Monteith equation, adapted from Shuttleworth and Wallace (1985) to determine canopy bulk surface resistance, $r^c_{s.PMSW}$:

$$r^c_{s.PMSW} = \frac{\Delta(r_a^a + r_a^c)(N - \lambda E_c) + \rho_a C_p D - \Delta r_a^c N_s}{\lambda E_c \gamma} - (r_a^c + r_a^a) \qquad (3)$$

where Δ is the rate of change of saturation vapor pressure with temperature (Pa K^{-1}), γ is the psychrometric constant, (Pa K^{-1}), C_p is air specific heat at constant pressure (J kg^{-1}K^{-1}), ρ_a is air density (kg m^{-3}) and D is vapor pressure deficit (Pa) at reference height. N is total available energy for turbulent fluxes (defined as $R_n - G$ in W m^{-2}), while N_s is the available energy for turbulent fluxes from soil; assumed as not less than 70% of N due to the observed clumping of tree's canopy which allows a high ratio of short wave radiation transmission. The term N_s is integrated in the equation because the soil energy budget can affect canopy temperature, thus canopy transpiration rate, thereby incorporating the interaction of both soil and canopy substrates into the model. Finally, E_c is the canopy transpiration rate (mm s^{-1}).

Calculations of r_a^c, with the respective stability corrections for momentum and heat transfer were taken from Paulson (1970). Further description of r_a^c calculation can be found in Appendix B.

Resistance for turbulent transport from source to screen height, r_a^a, is developed in Appendix C.

Once $r_{s.PMSW}^c$ is obtained from Eq. (3) it is possible to invert $r_{s.PMSW}^c$ in order to get canopy conductance. Additionally, conductance was expressed in mmol H_2O m^{-2} s^{-1} for its physiological, rather than physical, interpretation following Grace et al. (1995):

$$g_c = \frac{P}{\Re T r_{s.PMSW}^c} \tag{4}$$

where g_c is canopy conductance for water vapor in mmol H_2O m^{-2} s^{-1}, $\Re$ is the gas constant (8.31 J mol^{-1} K^{-1}), P is the air pressure expressed in Pa and T is air temperature in K.

We discarded g_c values that were 1.5 standard deviations away from a 10-day running mean for each 30 min interval. Additionally, periods when λE_{eco} was underestimated from data obtained with the Eddy Covariance station, thus resulting in negative λE_c estimates, were also neglected.

2.2.4. Inversion of the Penman–Monteith equation

When assuming that λE_{eco} is only dominated by canopy's transpiration, it is possible to use the inversion of PM. In order to obtain $r_{s.PM}^c$ we applied a modified version of the Penman–Monteith equation taken from Allen et al. (1998). Considering *raa*, the manipulation of the equation yields:

$$r_{s.PM}^c = \frac{\Delta(r_a^a + r_a^c)(N - \lambda E_{eco}) + \rho_a C_p D}{\lambda E_{eco}\gamma} - (r_a^c + r_a^a) \tag{5}$$

where, $r_{s.PM}^c$ is the canopy resistance derived from the PM equation. Likewise, Eq. (4) was applied in order to express $r_{s.PM}^c$ in its ecophysiological form, g_c.

2.3. Ground-based leaf gas exchange measurements

We measured g_s with a leaf gas exchange analyzer (Li 6400, Licor, NE, USA) during six field surveys: on April 17th (end of the dry season), September 5th, September 12th and September 26th (wet season) of 2012 and two other surveys on January 18th and January 21st of 2013 (mid-dry season). For every survey we selected four different trees and from each one leaf at mid-crown height from four different shoots pointing towards North, East, South and West was measured, in order to represent whole canopy conditions. Trees were randomly selected from the area representing the largest fetch and g_s observations from each leaf were obtained hourly. Since *Acacia* leaves are smaller than Li-6400's leaf chamber, the area of each leaf was determined by planimetry at the laboratory to correct measurements. In order to scale up from g_s to g_c we applied (adapted from Lhomme, 1991):

$$g_c = g_s \times L_0 \tag{6}$$

In cases where stomata are present on both sides of the leaf, g_s is multiplied by two times L_0, however woody *Fabaceae* species tend to be hypostomatous (Gill et al., 1982)

2.4. Canopy conductance modeling with the Jarvis approach

The Jarvis Model (Jarvis, 1976) is a function of the response of g_c to individual environmental variables controlling both leaf transpiration and photosynthesis. Canopy conductance responses are normalized, yielding values from 0 to 1 as a function of the observed maximal canopy conductance, g_{cmax}. Values close to 0 are related to non-optimal conditions, whereas values close to 1 indicate the contrary. In our study, g_c was related to the following variables: T_l (°C), PAR (μmol m^{-2} s^{-1}), D_l (kPa) and SWC (m^3 m^{-3} or%). Albeit TDR placed at 0.1 m belowground do not represent *Acacia*'s water availability due to the deep root exploration system that the gender *Acacia* can achieve (Canadell et al., 1996), SWC was used as a proxy for soil moisture depletion throughout the season indicating a water stress factor.

The Jarvis model is summarized as follows:

$$g_c = g_{cmax} f_1(T_l) f_2(D_l) f_3(PAR) f_4(SWC) \tag{7}$$

where Functions 8–11 are expressed as:

$$f_1(T_l) = \frac{((T_l - T_{low})(T_{high} - T_l))^{\tau}}{((T_o - T_{low})(T_{high} - T_o))^{\tau}} \tag{8}$$

$$f_2(D_l) = \exp(-k_2 D_l) \tag{9}$$

$$f_3(PAR) = 1 - \exp(-k_3 PAR) \tag{10}$$

$$f_4(SWC) = \begin{cases} 0.4; SWC \le \theta_w \\ \dfrac{SWC - \theta_w}{\theta_c - \theta_w}; \theta_w < SWC \le \theta_c \\ 1; SWC > \theta_c \end{cases} \tag{11}$$

where T_{low}, T_o and T_{high} are the minimum, optimum and maximum temperatures for g_c. The τ parameter is calculated as:

$$\tau = \frac{T_{high} - T_o}{T_{high} - T_{low}} \tag{12}$$

Minimum temperature and T_{high} values were obtained from ground-based observations and summarized in Table 1. Furthermore, θ_w is the soil water content at wilting point when g_c reaches its minimum while θ_c is a critical soil water content level when g_c becomes maximum. Usually, g_c is assumed 0 when SWC goes below θ_w, however, as the soil moisture probes did not assess *Acacia*'s water content because of their shallow depth, the minimum value for f_4 was replaced by 0.4. This value comes from g_c ground based measurements during the dry season that show that at its lower threshold ($SWC \approx 5\%$) g_c never went under 40% of g_{cmax}. Optimum temperature; k_2; k_3; θ_w and θ_c were derived by minimizing:

$$\chi_{\min} = \sum \{g_c^{obs} - g_{c\,\max} f_1(T_l) f_2(D_l) f_3(PAR) f_4(SWC)\}^2 \tag{13}$$

where g_c^{obs} is the observed canopy conductance obtained from the PMSW model, the PM inversion or the set of ground-based observations depending on the calibration dataset. Because of the use of ground-based g_c observations obtained during the six surveys, only 30% of these measurements were used for the calibration with the remaining 70% kept for validation. Given the piecewise nature of f_4, parameters were obtained iteratively for θ_c and θ_w and then analytically for the remaining variables. Finally, the set of values for θ_c and θ_w that showed the lowest least square error when minimizing χ were kept along with the other parameters obtained through the optimization process. Given the nonlinear nature of Eq. (7); we used the least square non linear fitting function found in Matlab optimization toolkit (Mathworks, MA, USA) which is based on the Newton–Raphson method.

2.5. The Farquhar–Ball–Berry model

Ball et al. (1987) sought to model g_s by linking stomatal behavior to A_n outputs from the Farquhar et al. (1980) photosynthesis model, resulting in the Farquhar–Ball–Berry (FBB) model. These formulations are combined to estimate unstressed stomatal conductance, and species-specific control can be introduced in the model by modifying the slope of the Ball–Berry stomatal conductance relation (Baldocchi and Meyers, 1998).

Leaf carbon net assimilation was obtained according to Farquhar et al. (1980). Later, A_n was coupled to g_s following Ball et al. (1987):

$$g_s = g_{s0} + m\frac{A_n}{C_s} rh_s f_4(SWC) \tag{14}$$

Table 1
Canopy conductance temperature threshold used of the Jarvis model and parameters obtained from both field observations and literature for the Farquhar photosynthesis model and the Farquhar–Ball and Berry stomatal conductance model.

Variable	Value	Unit	Source
Jarvis multiplicative model			
T_{low}	13	°C	Field observation
T_{high}	37	°C	Field observation
Farquhar photosynthesis model			
R_d	7.14	μmol m^{-2} s^{-1}	Field observation
V_{cmax}	70.32	μmol m^{-2} s^{-1}	Field observation
J_{max}	125.71	μmol m^{-2} s^{-1}	Field observation
Γ_p^*	35	μmol mol^{-1}	Su et al. (1996)
K_c	274.6	Dimensionless	Su et al. (1996)
K_o	419.8	Dimensionless	Su et al. (1996)
Enthalpy term	200	kJ mol^{-1}	Su et al. (1996)
Entropy term	0.71	kJ K^{-1} mol^{-1}	Su et al. (1996)
Activation energy for electron transport	55	kJ mol^{-1}	Su et al. (1996)
Activation energy for carboxylation	55	kJ mol^{-1}	Su et al. (1996)
Farquhar–Ball and Berry g_s model			
g_{s0}	2.28	mmol H_2O m^{-2} s^{-1}	Statistical fitting
m	11.4	mmol H_2O m^{-2} s^{-2} (μmol CO_2 m^{-2} s^{-1})$^{-1}$	Statistical fitting
R^2 regression	Dimensionless	Statistical fitting	

where C_s is the CO_2 concentration on the leaf surface, g_{s0} is the residual g_s that a leaf would achieve when A_n is zero and m is the change rate of g_s depending on A_n representing the composite stomatal sensitivity to A_n, C_s and relative humidity at the leaf surface (rh_s). We followed the procedure proposed by Su et al. (1996) to calculate C_s, rh_s and finally to compute A_n through a cubic equation from the same work. The V_{cmax} and J_{max} parameters for the Farquhar model were obtained from both A_n/C_i and A_n/PAR curves, made from eight different leaves on August 2013, using the method proposed by Sharkey et al. (2007). Since total stomatal behavior represents the combined above and belowground influences, we corrected the original FBB equation estimates by soil water availability, multiplying the FBB outcomes by the water restriction function, $f_4(SWC)$ (Eq. (11)) obtained through the calibration with ground-based measurements. Similar integration of water restriction on the FBB model can be found in Van Wijk et al. (2000) and Keenan et al. (2010).The Ball–Berry formulation for g_s was parameterized using field measurements of leaf H_2O and CO_2 exchange. By plotting $A_n/C_s \times (rh_s f_4(SWC))$ against g_s ground-based measurements it was possible to obtain g_{s0} and m through a linear statistical fitting of the data using Matlab (Mathworks, MA, USA). Ground-based g_s measurements used for the linear fitting were obtained from the same subset of 30% of the total amount of observations used to calibrate the Jarvis model with ground-based observations in order to avoid circularity with the validation set. Table 1 shows the parameterization obtained as a result of this procedure. Finally, in order to compare FBB outputs with those from the Jarvis, g_s was upscaled to g_c by applying Eq. (6). For all models, each interval with R_n values below 10 W m^{-2}, g_c was assumed zero because of the low PAR availability for photosynthesis.

2.6. Measuring multiplicative model accuracy against each calibration set and their further performance in the field

In order to assess multiplicative model's accuracy we determined model efficiency (ME) for each calibration set. Model efficiency was obtained following Whitley et al. (2013):

$$ME = 1 - \frac{\sum (Y_i - f(X_i, \beta))^2}{\sum (Y_i - \bar{Y})^2} \quad (15)$$

where the numerator represents the variance of the model ($f(X_i,\beta)$) against the calibration data set (Y_i) and the denominator represents the variance of the calibration set itself. Model efficiency can range between $-\infty$ and 1; a value of 1 indicates a perfect matching between the variance of the model and the calibration set, while a ME close to 0 indicates that the variance of the model and the one of the calibration set are similar, resulting in the mean of the observation being as good as the model to predict any observed value of g_c (Whitley et al., 2013).

In order to determine if the parametrs obtained with the PMSW or PM calibration set were different from each other, we perform a t-student difference mean test with an α value of 0.05 using Matlab (Mathworks, MA, USA). The standard deviations needed for the test were obtained by running five subsets for each calibration set. We did not perform the same analysis with the ground-based calibration set given that the low amount of field observations ($n = 36$) were not enough to get five different subsets.

To account for all multiplicative and the FBB models performance against ground-based g_c observations, we determine the root mean square error (RMSE) for each model, given by:

$$\mathrm{RMSE} = \sqrt{\frac{(g_c^{obs} - g_c^{\mathrm{mod}})^2}{n}} \quad (16)$$

where the numerator is the difference between model output, g_c^{mod}, and ground based-observation, g_c^{obs}, all divided by the number of observations, n.

2.7. Ecosystem heterogeneity determination by ^{13}isotopic discrimination

Because the fetch area of the Eddy Covariance station varies depending on wind speed, it becomes important to acknowledge that part of the fluxes could come from other areas of the Savannah, different from where ground-based g_c measurements for model's validation were obtained. We sampled *A. caven* in an upwind transect for ^{13}C isotopic discrimination in order to assess how heterogeneous the Savannah was respect to g_c (Farquhar et al., 1989). In April 2012, by the end of the dry season, healthy green leaves from year's growth were collected from four trees over four different plots across the transect and then immediately dried back at the laboratory at 65 °C until weight variation was no longer observed. Leaves were collected from mid-crown in all possible directions. Samples were smashed and then homogenized by plot. Ten samples per plot were sent to UC Davis Stable Isotope Facility (Davis, CA, USA) for ^{13}C natural abundance analysis. Stable carbon isotopes

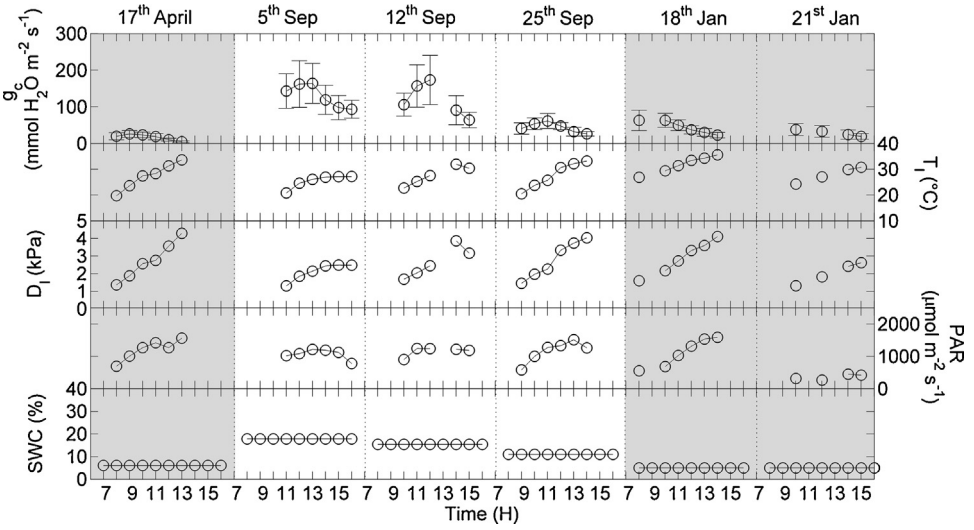

Fig. 3. Canopy conductance (g_c) evolution in *Acacia caven* along six field surveys performed on April the 17th, September the 5th, 12th and the 25th, 2012 and January the 18th and 21st, 2013. Canopy conductance observations represent hourly averages from four different mid-crown leaves pointing towards North, East, South and West in four different trees (16 leaves per hour). Canopy conductance observations are presented with its corresponding standard deviation together with leaf temperature (T_l), leaf-to-air water vapor deficit (D_l), photosynthetically active radiation (*PAR*) and soil water content (*SWC*). On gray background, surveys corresponding to the dry season while on white, surveys corresponding to the wet season.

values were expressed relative to the international standard Vienna PeeDee Belemnite, VPDB, ($\delta^{13}C_{VPDB}$).

3. Results and discussion

3.1. Seasonal evolution of canopy conductance

Fig. 3 shows the behavior of the mean values of g_c and other environmental variables (T_l, D_l, PAR and *SWC*) obtained at different hours during the six field campaigns. Each day, g_c showed the expected diurnal behavior: maximum g_c daily values were observed during the morning following an increase in *PAR*, thereafter, together with high midday values of T_l and D_l, g_c started declining, avoiding excessive water loss potentially leading to hydraulic failure. This strategy improved *Acacia's* water use efficiency, as has been previously reported for this type of vegetation (Flexas et al., 2014). At a seasonal level, g_c observations showed a synchronism with ecosystem water availability: larger g_c values were found when *SWC* was in its higher threshold (*SWC* > 15%). On the other hand, lowest g_c values were observed on April the 17th, at the end of the 2011–2012 dry season, when soil moisture was expected to be almost entirely depleted after summer evapotranspiration and the lack of rainfall since the previous winter (*SWC* ≈ 5%). This day was also characterized by high T_l and D_l values, thus compromising stomatal opening (Fig. 3). During the month of September (wet season), g_c values were higher following the increase in *SWC*. Maximum observed g_c, was observed on September the 12th at midday, with a value of ≈175 mmol H_2O m^{-2} s^{-1}. Even though the field survey of 25th September was performed during the wet season, g_c values were not as high as the ones achieved two weeks earlier, which can be attributed to high D_l values, which compromised leaf gas exchange. Moreover, by this date, *SWC* started to decay, indicating the transition to a new dry season. This synchronicity between *SWC* and gas exchange in savannahs dominated by *Acacia* has been also observed in *A. mulga* in Central Australia (Cleverly et al., 2013). However, in Australia the situation is reversed. Given the convective nature of their storms, major rain pulses are observed during the summer along with high evaporative demand. *A. mulga* also depends on soil water storage for gas exchange, however the time lag between high evapotranspiration and soil storage recharge is shorter since it occurs during the same season. This highlights *A. caven* control over its gas exchange capacity to deal with low water potential for a longer time.

Furthermore, two other surveys were performed on January 2013 (mid dry season). Even though they were only three days apart from each other, g_c values from the 21st January were relatively lower compared to the values obtained on the 18th January. The survey of the 21st January was chosen because a cloudy day was forecasted allowing to test g_c under low *SWC* and *PAR*. As expected, g_c showed a negative response to low light beyond restrictions imposed by low *SWC* as shown by lower values compared to g_c observations from the clear sky conditions of 18th January.

3.2. Jarvis model fitting and simulation

The Jarvis model was obtained by fitting Eq. (13) to three g_c data sets obtained from: (1) PMSW, (2) PM and (3) a set of ground-based measurements. Table 2 shows the parameters for g_{cmax}, T_{opt}, k_2, k_3 and θ_w, θ_c obtained for each calibration set. When comparing statistical differences between the parameters obtained with the PMSW and the PM set, only k_2, which computes the response of g_c to D_l, and θ_w proved to be different (P value < 0.001 in both cases). Because the PM data set considers whole ecosystem evapotranspiration, rather than just tree's transpiration, we believe that during the dry season together with higher D_l and lower λE_{bs} (due to the lack of an understory), k_3 exerts a higher penalty over g_{cmax} (Fig. 4). Even if the k_3 obtained with PM is closer to the one obtained with the ground-based data set, this could be due to the fact that the ground-based data set is not a good estimator for representing the transition between the two seasons; because field measurements were taken either during the wet or during the dry period. Thus, the ground-based data set is dominated by high D_l and low g_{cmax} resulting in a higher penalty given by k_2. On the other hand, θ_w obtained with the PM dataset was lower than the one obtained with the PMSW calibration, as the understory is more sensible to changes in *SWC* because of its shallow root system when compared to *A. caven*. Therefore, when *SWC* reaches its lower threshold λE_{bs} falls close to 0, thus affecting g_{cmax} estimations for the PM dataset.

Regarding ME, both the PMSW and the PM showed similar efficiencies close to 0, indicating that the variance of the method is

Table 2
Parameters obtained for the Jarvis model with the inversion of the Penman–Monteith equation in combination with the Shuttleworth and Wallace model for evapotranspiration from sparse canopies (PMSW), the inversrion of the Penman–Monteith equation (PM) and ground-based measurements, standard deviation for each parameters are shown in parenthesis. Statistical difference between parameters between the PMSW and PM calibration set were obtained with a *t*-student test at an α value of 0.05; parameters that resulted to be different are shown with ***. Accordingly, the *P* value for the probability of PMSW parameter is equal to the PM parameter is also displayed together with model efficiency (ME) and the number of observation used for the calibration (*n*).

Parameters	PMSW	PM	Statistical difference	*P* value	Ground-based
g_{cmax}	125 (30.3)	129 (15.74)		$P>0.01$	196
T_{opt}	29.57 (6.28)	20 (0.01)		$P>0.01$	33
k_2 (D_l)	0.096 (0.082)	0.401 (0.05)	***	$P<0.001$	0.38
k_3 (*PAR*)	0.013 (0.003)	0.005 (0.002)		$P>0.01$	0.002
θ_w (*SWC*)	8.6 (0.89)	5 (0.22)	***	$P<0.001$	6.7
θ_c (SWC)	20.8 (7.14)	27.4 (3.00)		$P>0.01$	15.5
Fitting					
ME	−0.04	0.02			0.37
n	4787	3868			36

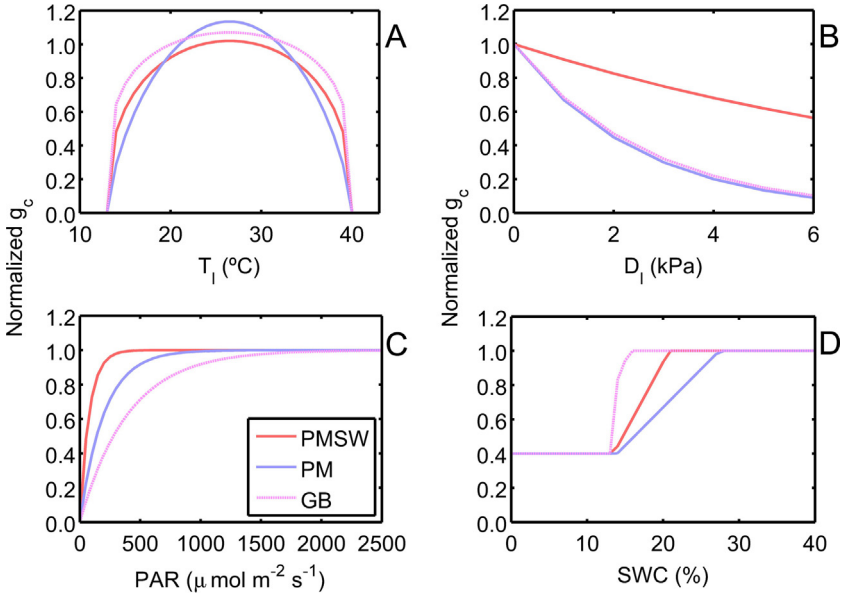

Fig. 4. Response function for the Jarvis model for (A) leaf temperature (T_l), (B) leaf-to-air water vapor deficit (D_l), (C) photosynthetically active radiation (*PAR*) and (D) soil water content (*SWC*). Obtained response functions are shown for the inversion Penman–Monteith equation in combination with the Shuttleworth and Wallace model for evapotranspiration from sparse canopies (PMSW), the inversion of the Penman–Monteith equation (PM) and the groud-based (GB) calibration set.

similar to the variance of the calibration data set. Only the model calibrated with ground-based g_c measurements showed an efficiency closer to 1, reflecting a high accuracy between the model and the calibration set. Nevertheless, the ground-based data set only comprises 36 observations, compared to the 4787 and 3868 observations for the PMSW and PM, respectively. Even if we used two different subsets for the calibration and validation process we cannot rule out circularity.

Fig. 5 shows hourly estimated g_c mean values for each month from October 2011 to January 2013 for the three Jarvis and the FBB models. All models generally predicted lower g_c values during the first dry season (October 2011–April 2012). *Acacia*'s predicted g_c by all models declined after October 2012 together with soil moisture. Even though these months presented a decrease in g_c, predicted values were not as low as the ones obtained during the October–December 2011 period. This may be due to the fact that 2011 reported 103 mm of total precipitation, whereas 2012 almost doubled that amount with 198 mm. This increase in 2012 precipitation could have been enough to enhance g_c due to greater soil water availability in deeper layers, thus allowing larger g_c at the beginning of the dry season. Also, all models show an increase in g_c during December 2012. This can be attributed to a 12 mm rainfall on the 19th Dec, which may have affected *SWC*. Nevertheless, a decrease of predicted g_c over January 2013 was observed, indicating that December's rain effect was attenuated because of typical summer high evaporative demand, which rapidly depleted soil moisture.

All models demonstrated a water stress avoidance mechanism by *A. caven*, in order to cope with water stress during the dry season (Chaves et al., 2002). As expected, *A. caven* showed an isohydric behavior (Galmés et al., 2007). During the months of maximum soil water stress, g_c control was tighter, thus, maintaining plant water status and thereby maintaining minimal metabolic functioning allowing plant survival at the expense of carbon gain (Tardieu and Simonneau, 1998). Moreover, possible high nitrogen concentration in *Acacia* leaves due to its leguminous nature would enhance photosynthetic performance, thus improving water use efficiency during the short periods of time that plant water status allowed stomatal opening (Reich, 2014; Wright et al., 2005). In fact, Niinemets et al. (2004) measured V_{cmax} in several European Mediterranean species such as *Quercus coccifer*, *Q. faginea*, *Q. ilex* and *Q. suber*, none of those species exceeded a value of 60 μmol m^{-2} s^{-1} while *A. caven* showed a value of 70.32 μmol m^{-2} s^{-1}. Accordingly, *Acacia ligulata* and *A. mangium* in Australia reached values of 67 and 62 μmol m^{-2} s^{-1}, respectively (Wullschleger, 1993), possibly explaining an enhanced photosynthetic performance because of nitrogen fixation. At an ecosystem level, Eamus et al. (2013) observed a similar behavior,

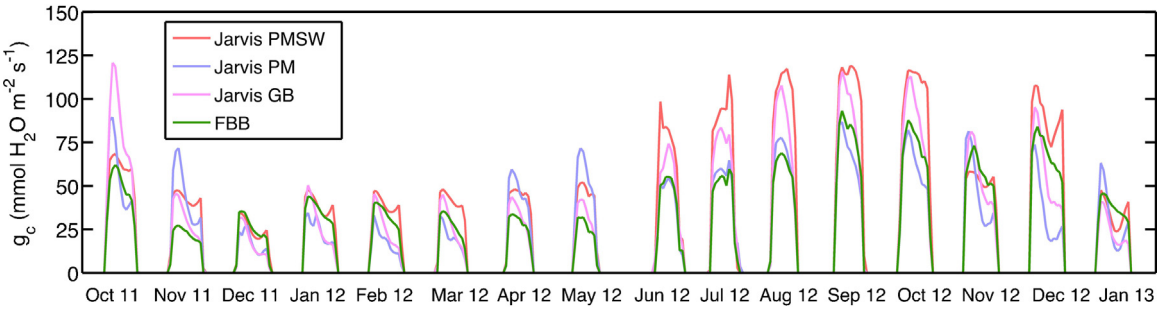

Fig. 5. Average hourly estimated canopy conductance (g_c) for *Acacia caven* for each month, from October 2012 to January 2013, obtained by: the Jarvis Model calibrated with the g_c inversion of the Penman–Monteith equation in combination with Shuttleworth and Wallace model for evapotranspiration from sparse canopies (Jarvis PMSW) data set, the g_c inversion of the Penman–Monteith equation data set (Jarvis PM), g_c ground-based measurement (Jarvis GB) and the Farquhar–Ball–Berry (FBB) for stomatal conductance scaled up to g_c.

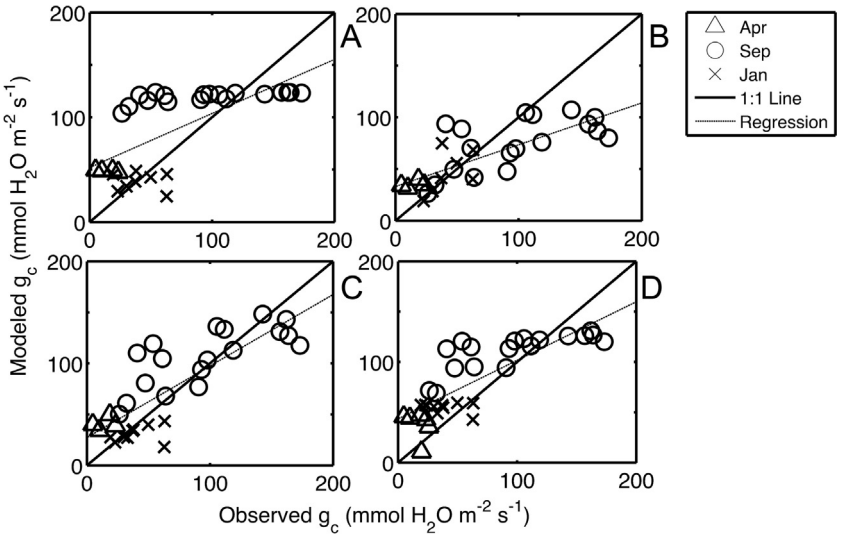

Fig. 6. Comparison between modeled canopy conductance (g_c) through: (A) the Jarvis model calibrated with the Penman–Monteith equation with the Shuttleworth and Wallace model for evaporation from sparse canopies (PMSW), (B) the inversion of the Penman–Monteith equation, (C) a set of g_c ground-based measurements and (D) the Farquhar–Ball–Berry (FBB) g_s model scaled up to the canopy level, against hourly g_c field observations obtained with a leaf gas analyzer. Each observation represents the average of 16 leaves measurements obtained during one survey on April, three on September 2012 and two surveys on January 2013 except for the Jarvis model calibrated with ground-based measurements and the FBB model, where, in order to avoid auto-correlation a random subset of 30% was used for model's parameterization whereas the remaining 70% was used for validation.

higher water use efficiency in a savannah dominated by *A. mulga* was achieved when *SWC* was lower, thus indicating a higher control on transpiration by stomatal constrains, which improved the relationship between carbon gain and water loss.

3.3. Models performance as tested with ground-based measurements

Fig. 6 shows the Jarvis model calibrated with the PMSW, PM and ground-based g_c measurements against the validation set. The inversion of the PM equation has been used to determine g_c on continuous canopies by Grace et al. (1995) and Harris et al. (2004), both cases in the Amazon forest. On the other hand, Lhomme and Monteny (2000) already used the PMSW model to derive flux partitioning in semi-arid ecosystems, however in this case, g_c was coupled to ecosystem's latent heat flux partitioning rather than λE. Lhomme and Monteny (2000) model was also tested against ground based g_c measurements showing a high correlation between observed and predicted values, thus endorsing ecosys-

Table 3
Statistical summary for all regression between modeled g_c obtained through the Jarvis model calibrated with the inversion of the Penman–Monteith equation in combination with the Shuttleworth and Wallace model for evapotranspiration from sparse canopies (PMSW), the Jarvis model calibrated with the inversion of the Penman–Monteith equation (PM), the multiplicative approach calibrated with ground-based measurements and g_c outputs from the Farquhar–Ball–Berry model (FBB). A FBB model without a penalty factor for soil water content (SWC) is also presented. Root mean square error (RMSE) and Model efficiency (ME) for each model are also displayed.

	PMSW	PM	Ground-based	FBB	FBB without SWC control
Intercept	51.95	33.02	27.37	43.56	109.615
Slope	0.52	0.41	0.7	0.58	0.057
P value	<0.005	<0.005	<0.005	<0.005	0.474
R^2	0.45	0.57	0.67	0.67	0.319
n	30	29	31	39	39
RMSE	43.18	39.41	32.67	33.61	68.11
ME	0.31	0.48	0.65	0.55	−0.86

tem's flux partitioning to obtain g_c in sparse canopies to be later on used for others models calibration purposes.

Table 3 shows a summary of the statistical performance of all of our models against the validation dataset. When comparing the outputs from the Jarvis model calibrated with the g_c obtained from λE fluxes, the PMSW presented a slightly higher RMSE (43.18 mmol H_2O m^{-2} s^{-1}) when compared to the Jarvis outputs obtained through the PM calibration (RMSE = 39.41 mmol H_2O m^{-2} s^{-1}). Even though both performances were similar we would not recommend the use of PM based on the big leaf approach to obtain g_c or g_s. The similar performance of these models could be explained by the fact that maximum canopy transpiration rate were similar to soil's evapotranspiration rates during the wet season given the presence of an understory. Thus, g_{cmax} values obtained from the optimization process were similar in magnitude (Table 2). However, if both soil and crown evapotranspiration rates are not synchronized, using the big-leaf approach could render misleading conclusions. Furthermore, when deriving g_s from g_c by inverting Eq. (6), L_0 becomes crucial. Since the canopy and understory could have different L_0 values, when obtaining g_s could be different when comparing simulated values to ground-based observations. The Jarvis model calibrated with the PMSW showed a consistent overestimation of predicted g_c in September. Overestimated values correspond to the last survey during this month that was characterized by high D_l values. It may be that the overestimation of g_c is due to the lower penalty that the factor k_2 regarding D_l that the model calibrated with the PMSW data set presented. On the other hand, g_c values obtained with the PM data set shows a consistent underestimation for high g_c values, this is explained because the calibration with this dataset arose the highest value for θ_c, the last could results in an underestimation of g_c during the wet season, when canopy transpiration is expected to be high.

The best agreement between observed and modeled g_c was achieved by the Jarvis model calibrated with the ground-based data set with a RMSE of 32.67 mmol H_2O m^{-2} s^{-1}, demonstrating the importance of this kind of intensive measurements to simulate ecophysiological traits. Even though the data sets obtained by the PMSW and PM methods contained an indirect measurement of g_c throughout the season, ground-based measurements significantly improved model's performance. However, these measurements are only useful when representing as much as possible of the ecosystem (several trees) and when they are obtained under different environmental conditions in order to represent g_c evolution throughout the year and its consequent seasonality.

The FBB showed a similar performance compared to the Jarvis model calibrated with the ground-based data set (RMSE of 33.61 mmol H_2O m^{-2} s^{-1}) Furthermore, differences between dry and wet season surveys were achieved by the FBB, revealing the importance of integrating soil moisture into canopy-atmosphere exchange models in arid and semi-arid ecosystems. To prove this, we compared the performance of the FBB with and without the water restriction (f_4) penalty (Fig. 7) against the ground-based g_c validation set. Best agreement (RMSE = 33.61 mmol H_2O m^{-2} s^{-1}) was obtained by implementing the water restriction penalty, when the penalty was not applied the performance of the model was considerably lower (RMSE = 64.01 mmol H_2O m^{-2} s^{-1}) because of an overestimation of g_c during the dry season (Table 3). This reinforces the importance of integrating soil moisture over canopy exchange in species presenting an isohydric behavior. However, *SWC* was determined by TDR probes placed at 0.1 m depth, without accounting for *Acacia*'s access to water in deeper soil layers. As suggested by Rambal et al. (2003), *SWC* in superficial layers does not entirely represent water availability in arid vegetation, making predawn leaf water potential or deep soil moisture assessment (below 4 m) a better option to model this kind of ecosystems. However, predawn leaf water potential measurements in long-term studies are both

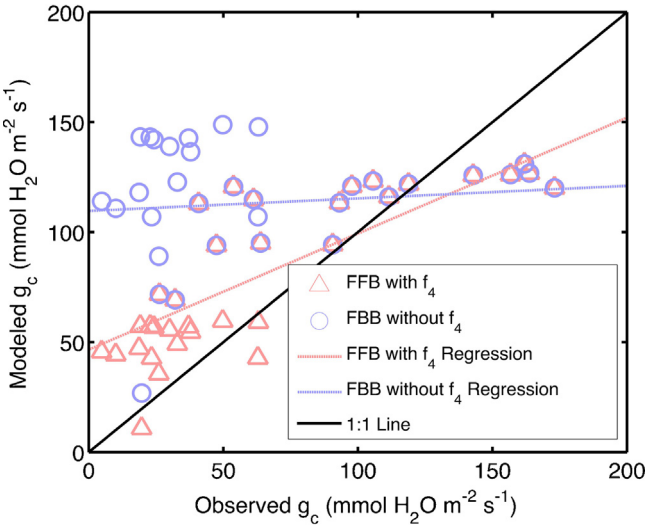

Fig. 7. Comparison of the Farquhar-Ball-Berry (FBB) stomatal conductance model scale up to canopy conductance (g_c) with and without a water restriction factor (f_4) in order to account for *Acacia caven* isohydric behavior.

demanding in time and effort. Nevertheless, integrating *SWC* in the model allowed to improve seasonal response of g_c as compared to only accounting g_c response to D_l as a water stress indicator (*e.g.*: Law et al., 2001).

Moreover, other considerations for models relying on photosynthetic performance, like the FBB approach, must be addressed. The carbon dioxide flux from the surrounding air to the carboxylation site not only depends on leaf's g_s and the boundary layer conductance (g_b) but also on the conductance of the internal medium of the leaf to carbon, known as mesophyll conductance (g_m) (Flexas and Medrano, 2002) which, together with the former two conductances, determines CO_2 concentration in the carboxylation sites (C_c). Drought conditions increase non-stomatal limitation to photosynthesis by partially decreasing g_m through the diminishing of both carbonic anhydrase and aquaporins activity, together with lignification of the cell wall (Flexas and Medrano, 2002). In this sense, the relationship between C_i and C_c will not be constant because the former depends on both g_b and g_s, and the latter (which actually drives photosynthesis) also depends on g_m. This leads to a decoupling of the relationship between A_n and g_s upon which the FBB approach is based on. The former highlights the need of adding g_m into the FBB model when predicting stomatal behavior in Mediterranean ecosystems (*e.g.*: Keenan et al., 2010; Zhou et al., 2013). However, iterating for an optimal solution that satisfies A_n, g_s, g_m and C_s is challenging and not always possible.

The multiplicative approach is the result of the partial contribution of each variable to stomatal behavior, thus neglecting the effect of their interaction over g_c. As climate change remains a challenge to understanding the future of ecosystem's exchange, it becomes important to integrate these synergies into stomatal response in Dynamic Global Vegetation Models (Ainsworth and Rogers, 2007). These challenges stress the urge to develop mechanistic models able to refine the estimation of g_s and its upscaling to g_c as these are the only models that can simulate stomatal response under a new range of environmental conditions (higher atmospheric CO_2 concentrations and T_l; and lower *SWC*). However, the simplicity and good agreement of the multiplicative approach have led it to be part of larger models, such as functional structural models (*e.g.*: Dauzat et al., 2001).

In turn, the FBB model is the closest to a mechanistic approach, as its performance relies upon A_n. However, physiological parameters have proven to vary with the season. Xu and Baldocchi (2003)

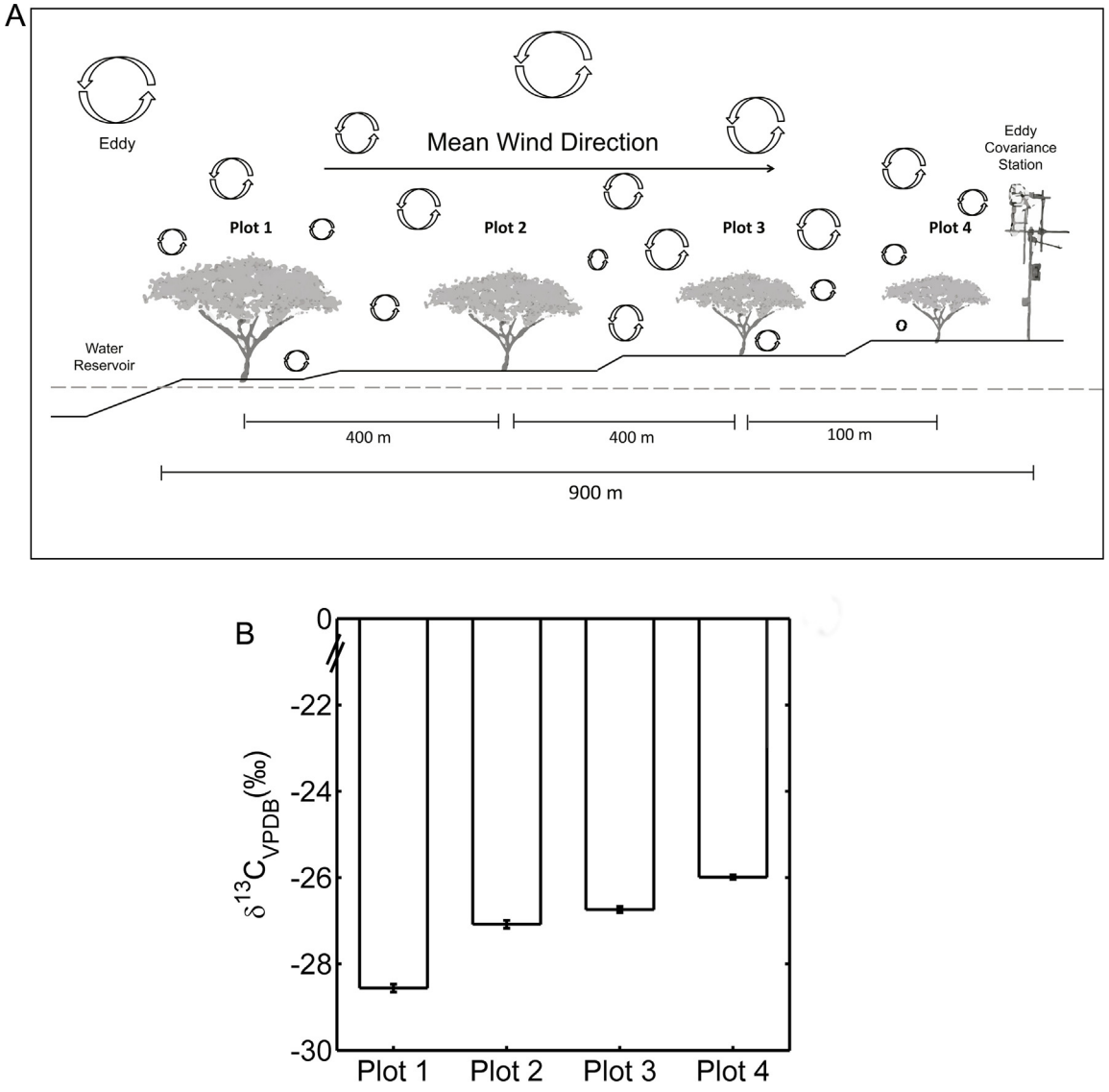

Fig. 8. In A, diagram of the four plots sampled for *Acacia caven* stable Carbon istope discrimination, $\delta^{13}C_{VPDB,}$ and how an increase in mean wind speed could increase the fetch area by dragging eddies from a farther distance in the upwind direction. Tree's size represents the observed vigor trend of each plot. In B, $\delta^{13}C_{VPDB}$ results for each plot. As plots become closer to the water reservoir, $\delta^{13}C_{VPDB}$ values increase, suggesting larger stomatal conductance over the season, thus representing high heterogeneity in the savannah.

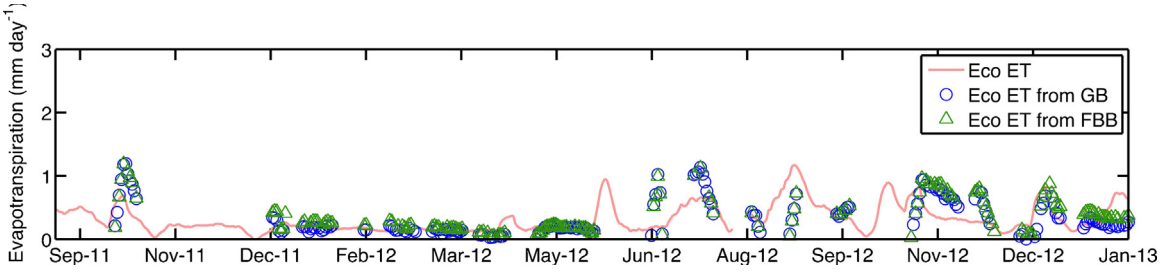

Fig. 9. Ecosystem evapotranspiration rates (Eco ET) obtained from the Eddy covariance station along with modeled ecosystem evapotranspiration using the Penman–Monteith equation together with the Shuttleworth and Wallace model for sparse canopy latent heat, using g_c outputs from the Jarvis model calibrated with ground-based measurements (Eco ET from GB) and estimated ecosystem evapotranspiration rates using the outputs of the Farquhar–Ball–Berry canopy conductance model (Eco ET from FBB), both of them transformed to their resistances terms.

demonstrated that both V_{cmax} and J_{max} rates in *Quercus douglasii* (a schlerophyllous evergreen much like *A. caven*), under prolonged drought conditions showed a decay after the period of maximal A_n, following a decrease in plant water status and the beginning of extreme conditions for the plant, such as high T_l, thus making model parameterization demanding.

3.4. Canopy conductance: scaling challenges

When calibrating an empirical model with indirect g_c measurements, such as the PMSW, PM equation or sap flow measurements, it becomes important to acknowledge that these are local measurements, given by a certain area of fetch in the case of Eddy Covariance, or the selection of trees where sap flow meters are placed (Whitley et al., 2013). Hence, these models do not always represent entire ecosystem conditions. A high heterogeneity regarding *Acacia* vegetative vigor was observed in the field. This could be attributed to the fact that 800 m in the upwind direction from the area of maximal fetch, a small water reservoir was filled for irrigation purposes, thus increasing soil moisture through the transect between the water body and the Eddy Covariance station (Fig. 8A). Even though none of our footprint models estimated a direct influence of evaporation from the reservoir over λE_{eco}, *Acacia's* water availability could largely vary within the transect, thus leading to a high variation of λE_c and consequently of g_c. In order to evaluate differences in long term gas exchange across the transect, we assessed general stomatal behavior by ^{13}C discrimination ($\delta\ ^{13}C$) (Farquhar et al., 1989).

Lower values for $\delta^{13}C_{VPDB}$ reflect greater C_i availability due mostly to a larger g_s, thus indicating a better plant water status in this kind of vegetation (Ortiz, 2010). Plots with greater water availability showed higher $\delta^{13}C_{VPDB}$ values (Fig. 8B). Together with an increase in wind speed, the fetch area is also supposed to enlarge, thus flux data would show the influence from the plots that are farther away from the Eddy Covariance Station and closer to the water body. Savannahs, and other ecosystems as well, can present different soil and water capacity conditions, thus resulting in a high heterogeneity (Augustine, 2003).

Whitley et al. (2013) found, while calibrating a multiplicative model for ecosystem's transpiration across a series of different biomes, that response parameters to environment changed very little indicating that, even if the ecosystems were different, the response to available radiation (a proxy for *PAR*) and D_l was the same. However, main differences were found regarding maximal transpiration rate, a proxy for g_{cmax}, and soil water status. According to these findings, the present study could be extrapolated to the rest of Chile's Mediterranean region. Nevertheless, factors such as *SWC* and variation in g_{cmax} (probably reflected in Carbon isotopic discrimination) should be accounted in order to include spatial variability across the region.

Another important difference between the models is that they rely on different approaches. The FBB model and the ground-based measurements were scaled up to a canopy level to obtain g_c, using a "bottom-up" approach. Following Eq. (6), a correct L_0 determination is essential. Filho et al., (1998) found that when obtaining g_s from λE, in other terms downscaling g_s from g_c following the inversion of Eq. (6), best agreement was achieved when assuming that only the fraction of the canopy receiving higher radiation levels is responsible for the majority of λE, instead of assuming that all crown's leaf area was contributing to canopy gas exchange. Owing to *Acacia's* porous crown architecture and its low leaf area, 70% of the canopy, according to field visual estimation, was always directly exposed to light. Thereby, the results presented in our study were obtained by assuming an effective L_0 of 0.7 instead of the original value of 1.0; resulting from correcting for dry season LAI by f_c.

When comparing g_c values obtained through the inversion of the PM equation in combination with PMSW, with g_c ground-based measurements, best fit was observed assuming an L_0 of 0.7 (data not shown), thus endorsing the use of effective L_0 rather than observed L_0.

In order to demonstrate that our models were able to reproduce the Savannah's λE behavior across the year we estimate ecosystem evapotranspiration rates by introducing our estimates of g_c derived from the Jarvis model calibrated with the data set of ground-based g_s observations and g_c estimations from the FBB model into the PMSW model, together with ecosystem's evapotranspiration rates. We did not perform the same analysis with the g_c obtained from the multiplicative approach calibrated with the PMSW and PM since these were derived from the Eddy covariance station. Fig. 9 shows real and modeled evapotranspiration rates revealing *Acacia* isohydric behavior. Real and modeled fluxes show a high synchronicity with soil moisture given by the penalty function for *SWC*, thus highlighting the importance of incorporating soil water dynamics in this kind of vegetation in order to better account for the role of ecosystems in local and global basin water balances.

4. Conclusions

We modeled *A. caven* g_c behavior throughout the year following the Jarvis model calibrated with three different data sets (PMSW, PM and a set of ground-based measurements) and the FBB approach. Best agreement was achieved by the Jarvis model calibrated with g_c ground-based measurements. However circularity between the calibration and validation data set cannot be completely discarded. The semi-empirical FBB model also yield a good performance, indicating the importance of a mechanistic approach to better understand ecophysiological processes. The Jarvis model calibrated with the PM data set presented a slighter better performance than the one calibrated with the PMSW. However the big leaf approach is not always suggested to represent fluxes from sparse canopies.

We conclude that *A. caven* g_c showed a high synchronicity with environmental factors, such as *SWC* and D_l, explaining an elevated degree of water conservation given by a high control of water loss during the dry season. This trait is characteristic of Mediterranean vegetation, indicating an isohydric behavior. Following Whitley et al. (2013), these kinds of studies can be extrapolated to larger areas if differences between soil characteristics and g_{cmax} are accounted for. The use of a semi-empirical model improved g_c estimations, however, in the case of the FBB model, soil moisture effect over stomatal behavior must be integrated. Identifying the main environmental factors controlling g_c, and therefore gas exchange, in these ecosystems is of a great importance to understanding future feedbacks between climate change and carbon fluxes in arid and semi-arid regions. Furthermore, these results could enhance primary productivity models at a regional level or estimate natural ecosystems evapotranspiration rates, helping to improve both water balance estimation and management at a basin scale.

Acknowledgment

We would like to acknowledge the Chilean National Commission for Scientific and Technological Research (CONICYT) for sponsoring this research through the project Fondecyt 1090393 and the author's full scholarship. We would also like to thank Codelco División Andina for the use of the site, Dr. Felipe Bravo for his help regarding Eddy Covariance measurements and the suggestions of an anonymous reviewer that helped to improve the original manuscript.

Appendix A.

To obtain f_c, we analyzed Google Earth pictures from the Savannah on a 8 bits per pixel image gray scale. As every pixel presents a value raging from 0 to 255 (where a pixel with a value of 0 is black and a pixel with a value of 255 is white), values below a certain threshold, to represent tree crowns, were selected, following:

$$P(x,y) = \begin{cases} P(x,y) = 1; P(x,y) < \text{threshold} \\ P(x,y) = 0; P(x,y) > \text{threshold} \end{cases} \quad \text{(A.1a)}$$

$$f_c = \frac{\sum P(x,y)}{total\ number\ of\ pixels} \quad \text{(A.1b)}$$

In order to determine the value of the threshold, we selected an initial value and then we tried 50 random pixels. If most of the pixels non representing the canopy, according to a visual estimation, where being selected as part of the tree crown, we tried a slighty lower threshold until 90% of the 50 random pixels correctly determined a tree crown (reaching a value of 1) or bare soil (reaching a value of 0). Then, with the selected threshold we ran the analysis for 6 different images representing the area of maximal fetch, thus finally yielding f_c.

Appendix B.

Canopy aerodynamic resistance, r_a^c, was computed as follows. First, a tentative friction velocity was calculated following Foken (2008):

$$u_* = (cov\ uw^2 + cov\ vw^2)^{1/4} \quad \text{(B1)}$$

where u_* is the friction velocity (m s^{-1}) and *cov uw* and *cov vw* are the covariances between the wind speed in x and z axes and y and z axes respectively.

Then, Monin–Obukhov length was calculated as (Paulson, 1970):

$$m_0 = \frac{-u_*^3 C_p \rho_a T_v}{kgH} \quad \text{(B2)}$$

where k is the Von Karman constant (dimensionless), g is the gravitational acceleration of the Earth (m s^{-2}) and H is ecosystem sensible heat flux expressed in W m^{-2}. Finally, T_v is the virtual temperature in K, expressed as (Stull, 2000):

$$T_v = T(1 + 0.61r) \quad \text{(B3)}$$

where T is the air temperature in K and r is the mixing ratio.

After obtaining m_0 it is possible to obtain ζ to then calculate stability corrections for momentum (ψ_M) and heat (ψ_H) (Paulson, 1970):

$$\zeta = \frac{(z_r - d)}{m_0} \quad \text{(B4)}$$

where z_r is instrument reference height (m) and d is the zero plane displacement (m), assumed as 2/3 of h (Allen et al., 1998) while h is the mean canopy height (m). ψ_M and ψ_H are defined as:

$$\psi_M = \begin{cases} 2\ln\left(\frac{1}{2}(1+\zeta_0)\right) + \ln\left(\frac{1}{2}(1+\zeta_0^2)\right) - 2\arctan(\zeta_0) + \frac{\pi}{2}; \zeta \le 0 \\ -5\zeta_0; \zeta > 0 \end{cases} \quad \text{(B5.a)}$$

$$\psi_H = \begin{cases} 2\ln\left(\frac{1}{2}(1+\zeta_0^2)\right); \zeta \le 0 \\ -5\zeta_0; \zeta > 0 \end{cases} \quad \text{(B5.b)}$$

ζ_0 is defined as:

$$\zeta_0 = (1 - 16\zeta)^{1/4} \quad \text{(B6)}$$

Now, a second u_* estimation can be achieved following:

$$u_* \frac{ku}{\ln\left(\frac{z_r - d}{z_0}\right) - \psi_M} \quad \text{(B7)}$$

u is the main wind speed at z_r (s m^{-1}) and z_o is the roughness height for heat transfer, defined as $0.1 \times z_{ot}$.z_{ot} is the roughness height for momentum transfer, calculated as $0.123 \times h$, all of them expressed in m.

After correcting u_* it is possible to estimate canopy's aerodynamic resistance, r_a^c, with its stability corrections (Harris et al., 2004):

$$r_a^c = \frac{u}{u_*^2} + \frac{1}{ku_*}\left(\ln\left(\frac{z_o}{z_{ot}}\right) + \psi_M - \psi_H\right) \quad \text{(B8)}$$

Appendix C.

Resistance for turbulent transport from source to screen height, r_a^a, is calculated following Shuttleworth and Wallace (1985):

$$r_a^c = \frac{\ln\left(\frac{z_r - d}{z_{ot}}\right)}{k^2 u} \times \left[\ln\left(\frac{z_r - d}{h - d}\right) + \frac{h}{n(h-d)} \times \left[\exp\left(n\left(1 - \frac{d - z_{ot}}{h}\right)\right) - 1\right]\right. \quad \text{(C1)}$$

The only unknown term is n, the Eddy diffusivity decay, assumed as 2.5 according to Shuttleworth and Wallace (1985).

References

Ainsworth, E.A., Rogers, A., 2007. The response of photosynthesis and stomatal conductance to rising [CO_2]: mechanisms and environmental interactions. Plant Cell Environ. 30, 258–270, http://dx.doi.org/10.1111/j1365-3040.2007.01641.x

Allen, R.G., Pereira, L.S., Raes, D., Smith, M., 1998. Crop Evapotranspiration-Guidelines for Computing Crop Water Requirements-FAO Irrigation and Drainage Paper 56, First Ed. FAO, Rome, Rome, Italy.

Augustine, D.J., 2003. Spatial heterogeneity in the herbaceous layer of a semi-arid Savanna ecosystem. Plant Ecol. 167, 319–332.

Baldocchi, D., Meyers, T., 1998. On using eco-physiological, micrometeorological and biogeochemical theory to evaluate carbon dioxide, water vapor and trace gas fluxes over vegetation: a perspective. Agric. For. Meteorol. 90, 1–25, http://dx.doi.org/10.1016/S0168-1923(97) 72-5

Ball, J.T., Woodrow, I.E., Berry, J.A., 1987. A model predicting stomatal conductance and its contribution to the control of photosynthesis under different environmental conditions. In: Biggins, J., Nijhoff, M. (Eds.), Progress in Photosynthesis Research, Vol. 4. Proceedings of the 7th International Congress on Photosynthesis, Dordrecht, NE, pp. 221–224.

Berry, J.A., Beerling, D.J., Franks, P.J., 2010. Stomata: key players in the earth system, past and present. Plant Biol. 13, 233–240, http://dx.doi.org/10.1016/j.pbi.2010.04.013

Brenner, A.J., Incoll, L.D., 1997. The effect of clumping and stomatal response on evaporation from sparsely vegetated shrublands. Agric. For. Meteorol. 84, 187–205, http://dx.doi.org/10.1016/S0168-1923(96)2368-4

Canadell, J., Jackson, R., Ehleringer, J., Mooney, H., Sala, O., Schulze, E., 1996. Maximum rooting depth of vegetation types at the global scale. Oecologia 108, 583–595, http://dx.doi.org/10.1007/BF00329030

Chaves, M.M., Pereira, J.S., Maroco, J., Rodrigues, M.L., Ricardo, C.P.P., Osório, M.L., Carvalho, I., Faria, T., Pinheiro, C., 2002. How plants cope with water stress in the field. Photosynthesis and growth. Ann. Bot. 89, 907–916, http://dx.doi.org/10.1093/aob/mcf105

Cleverly, J., Boulain, N., Villalobos-Vega, R., Grant, N., Faux, R., Wood, C., Cook, P.G., Yu, Q., Leigh, A., Eamus, D., 2013. Dynamics of component carbon fluxes in a semi-arid *Acacia* woodland, central Australia. J. Geophys. Res. Biogeosci., http://dx.doi.org/10.1002/jgrg.20101

Cowling, R., Rundel, P., Desmet, P., Esler, K., 1998. Extraordinary high regional-scale plant diversity in Southern African arid lands: subcontinental and global comparisons. Divers. Distrib. 4, 27–36.

ORNL DAAC, 2014. MODIS subsetted land products, Collection 5 [WWW Document]. URL {\url{http://daac.ornl.gov/MODIS/modis.shtml}.

Damour, G., Simonneau, T., Cochard, H., Urban, L., 2010. An overview of models of stomatal conductance at the leaf level. Plant Cell Environ. 33, 1419–1438, http://dx.doi.org/10.1111/j.1365-3040.2010.02181.x

Dauzat, J., Rapidel, B., Berger, A., 2001. Simulation of leaf transpiration and sap flow in virtual plants: model description and application to a coffee plantation in Costa Rica. Agric. For. Meteorol. 109, 143–160, http://dx.doi.org/10.1016/S0168-1923(01) 236-2

Dewar, R.C., 2002. The Ball–Berry–Leuning and Tardieu–Davies stomatal models: synthesis and extension within a spatially aggregated picture of guard cell function. Plant Cell Environ. 25, 1383–1398, http://dx.doi.org/10.1046/j.1365-3040.2002.00909.x

Eamus, D., Cleverly, J., Boulain, N., Grant, N., Faux, R., Villalobos-Vega, R., 2013. Carbon and water fluxes in an arid-zone *Acacia* savanna woodland: an analyses of seasonal patterns and responses to rainfall events. Agric. For. Meteorol. 182–183, 225–238, http://dx.doi.org/10.1016/j.agrformet.2013.04.020

Farquhar, G., Ehleringer, J., Hubick, K., 1989. Carbon isotope discrimination and photosynthesis. Annu. Rev. Plant Physiol. 40, 503–537.

Farquhar, G.D., von Caemmerer, S., Berry, J.A., 1980. A biochemical model of photosynthetic CO_2 assimilation in leaves of C_3 species. Planta 149, 78–90.

Filho, J., Damesin, C., Rambal, S., Joffre, R., 1998. Retrieving leaf conductances from sap flows in a mixed Mediterranean woodland: a scaling exercise. Anne. des Sci. For. 55, 173–190.

Flexas, J., Diaz-Espejo, a., Gago, J., Gallé, a., Galmés, J., Gulías, J., Medrano, H., 2014. Photosynthetic limitations in Mediterranean plants: a review. Environ. Exp. Bot. 103, 12–23, http://dx.doi.org/10.1016/j.envexpbot.2013.09.002

Flexas, J., Medrano, H., 2002. Drought-inhibition of photosynthesis in C3 plants: stomatal and non-stomatal limitations revisited. Ann. Bot. 89, 183–189, http://dx.doi.org/10.1093/aob/mcf027

Foken, T., 2008. Micrometeorology, First Ed. Springer, Amsterdam, NE.

Galmés, J., Flexas, J., Savé, R., Medrano, H., 2007. Water relations and stomatal characteristics of Mediterranean plants with different growth forms and leaf habits: responses to water stress and recovery. Plant Soil 290, 139–155, http://dx.doi.org/10.1007/s11104-006-9148-6

Gao, Q., Zhao, P., Zeng, X., Cai, X., Shen, W., 2002. A model of stomatal conductance to quantify the relationship between leaf transpiration, microclimate and soil water stress. Plant Cell Environ. 25, 1373–1381, http://dx.doi.org/10.1046/j.1365-3040.2002.00926.x

Gill, L.S., Olabanji, G.O., Husaini, S.W.H., 1982. Studies on the structural variation and distribution of dtomata in some Nigerian legumes. Willdenowia, 87–94.

Grace, J., Lloyd, J., McIntyre, J., Miranda, A., Meir, P., Miranda, H., Moncrieff, J., Massheder, J., Wright, I., Gash, J., 1995. Fluxes of carbon dioxide and water vapour over an undisturbed tropical forest in south-west Amazonia. Global Change Biol. 1, 1–12.

Grouzis, M., Diouf, M., Rocheteau, A., Berger, A., 1998. Fonctionnement hydrique et réponses des ligneux sahéliens à l'aridité. In: Campa, C., Gringnon, C., Gueye, M., Hamon, S. (Eds.). L'Acacia Au Sénégal., Orstom, Paris, p. 476.

Harris, P.P., Huntingford, C., Cox, P.M., Gash, J.H.C., Malhi, Y., 2004. Effect of soil moisture on canopy conductance of Amazonian rainforest. Agric. For. Meteorol. 122, 215–227, http://dx.doi.org/10.1016/j.agrformet.2003.09.006

Jarvis, P.G., 1976. The Interpretation of the variation in leaf water potential and stomatal conductance found in canopies in the Field. Philos. Trans. R. Soc. Lond. B. Biol. Sci. 273, 593–610.

Keenan, T., García, R., Friend, A., Zaehle, S., Gracia, C., Sabate, S., 2009. Improved understanding of drought controls on seasonal variation in Mediterranean forest canopy CO_2 and water fluxes through combined in situ measurements and ecosystem modelling. Biogeosciences 6, 1423–1444.

Keenan, T., Sabate, S., Gracia, C., 2010. Soil water stress and coupled photosynthesis-conductance models: bridging the gap between conflicting reports on the relative roles of stomatal, mesophyll conductance and biochemical limitations to photosynthesis. Agric. For. Meteorol. 150, 443–453, http://dx.doi.org/10.1016/j.agrformet.2010.01.008

Kljun, N., Black, T.A., Griffis, T.J., Barr, A.G., Gaumont-Guay, D., Morgenstern, K., McCaughey, J.H., Nesic, Z., 2007. Response of net ecosystem productivity of three boreal forest stands to drought. Ecosystems 10, 1039–1055, http://dx.doi.org/10.1007/s10021-007-9088-x

Krishnan, P., Black, T.A., Grant, N.J., Barr, A.G., Hogg, E.H., Jassal, R.S., Morgenstern, K., 2006. Impact of changing soil moisture distribution on net ecosystem productivity of a boreal aspen forest during and following drought. Agric. For. Meteorol. 139, 208–223, http://dx.doi.org/10.1016/j.agrformet.2006.07.002

Law, B., Goldstein, A., Anthoni, P., Unsworth, M., Panek, J., Bauer, M., Fracheboud, J., Hultman, N., 2001. Carbon dioxide and water vapor exchange by young and old ponderosa pine ecosystems during a dry summer. Tree Physiol. 21, 299–308.

Lhomme, J., 1991. The concept of canopy resistance: historical survey and comparison of different approaches. Agric. For. Meteorol. 54, 227–240.

Lhomme, J., Monteny, B., 2000. Theoretical relationship between stomatal resistance and surface temperatures in sparse vegetation. Agric. For. Meteorol. 104, 119–131.

Liu, C., Zhang, X., Zhang, Y., 2002. Determination of daily evaporation and evapotranspiration of winter wheat and maize by large-scale weighing lysimeter and micro-lysimeter. Agric. For. Meteorol. 111, 109–120, http://dx.doi.org/10.1016/S0168-1923(02) 15-1

Mahrt, L., Pan, H., 1984. A two-layer model of soil hydrology. Boundary-Layer Meteorol. 29, 1–20.

Medlyn, B.E., Duursma, a, R., Eamus, D., Ellsworth, D.S., Prentice, I.C., Barton, C.V.M., Crous, K.Y., De Angelis, P., Freeman, M., Wingate, L., 2011. Reconciling the optimal and empirical approaches to modelling stomatal conductance. Global Change Biol. 17, 2134–2144, http://dx.doi.org/10.1111/j.1365-2486.2010.02375.x

Melillo, J., McGuire, A., Kicklighter, D., 1993. Global climate change and terrestrial net primary production. Nature.

Niinemets, Ü., Tenhunen, J.D., Beyschlag, W., 2004. Spatial and age-dependent modifications of photosynthetic capacity in four Mediterranean oak species. Funct. Plant Biol. 31, 1179–1193.

Ortiz, M., 2010. Nivel freático en la Pampa del Tamarugal y crecimineto de Prosopis tamarugo (Phil). Universidad de Chile, Santiago, Chile.

Otieno, D.O., Schmidt, M.W.T., Adiku, S., Tenhunen, J., 2005. Physiological and morphological responses to water stress in two *Acacia* species from contrasting habitats. Tree Physiol. 25, 361–371.

Paulson, C., 1970. The mathematical representation of wind speed and temperature profiles in the unstable atmospheric surface layer. J. Appl. Meteorol. 9, 857–861.

Pohlman, C., Nicotra, A., Murray, B., 2005. Geographic range size, seedling ecophysiology and phenotypic plasticity in Australian *Acacia* species. J. Biogeogr. 32, 341–351, http://dx.doi.org/10.1111/j.1365-2699.2004.01181.x

Rambal, S., Ourcival, J., Joffre, R., Mouillot, F., Nouvellon, Y., Reichsteins, M., Rocheteau, A., 2003. Drought controls over conductance and assimilation of a Mediterranean evergreen ecosystem: scaling from leaf to canopy. Global Change Biol. 9, 1813–1824, http://dx.doi.org/10.1046/j1529-8817.2003.00687.x

Reich, P.B., 2014. The world-wide fast-slow plant economics spectrum: a traits manifesto. J. Ecol. 102, 275–301, http://dx.doi.org/10.1111/1365-2745.12211

Reichstein, M., Tenhunen, J., Roupsars, O., Ourcival, J., Rambal, S., Miglietta, F., Peressotti, A., Pecchiari, M., Tirone, G., Valentini, R., 2002. Severe drought effects on ecosystem CO_2 and H_2O fluxes at three Mediterranean evergreen sites: revision of current hypotheses. Global Change Biol. 8, 999–1017.

Ryu, Y., Sonnentag, O., Nilson, T., Vargas, R., Kobayashi, H., Wenk, R., Baldocchi, D.D., 2010. How to quantify tree leaf area index in an open savanna ecosystem: a multi-instrument and multi-model approach. Agric. For. Meteorol. 150, 63–76, http://dx.doi.org/10.1016/j.agrformet.2009.08.007

Sharkey, T.D., Bernacchi, C.J., Farquhar, G.D., Singsaas, E.L., 2007. Fitting photosynthetic carbon dioxide response curves for C3 leaves. Plant Cell Environ. 30, 1035–1040, http://dx.doi.org/10.1111/j.1365-3040.2007.01710.x

Shuttleworth, W., Wallace, J., 1985. Evaporation from sparse crops-an energy combination theory. Q. J. R. Meteorolog. Soc. 111, 839–855.

Stewart, J., 1988. Modelling surface conductance of pine forest. Agric. For. Meteorol. 43, 19–35, http://dx.doi.org/10.1016/0168-1923(88) 90003-2

Stull, R., 2000. Meterology for scientists and engineers, Second Ed. Brooks/Cole, Pacific Grove, CA, USA.

Su, H.B., Paw, U.K.T., Shaw, R.H., 1996. Development of a coupled leaf canopy model for the simulation of plant-atmosphere interaction. J. Appl. Meteorol. 35, 748–773.

Tardieu, F., Simonneau, T., 1998. Variability among species of stomatal control under fluctuating soil water status and evaporative demand: modelling isohydric and anisohydric behaviours. J. Exp. Bot. 49, 419–432.

Tenhunen, J.D., Sala Serra, A., Harley, P.C., Dougherty, R.L., Reynolds, J.F., 1990. Factors influencing carbon fixation and water use by mediterranean sclerophyll shrubs during summer drought. Oecologia 82, 381–393, http://dx.doi.org/10.1007/BF00317487

Thom, A., 1972. Momentum, mass and heat exchange of vegetation. Q. J. R. Meteorolog. Soc. 98, 124–134.

Van Wijk, M.T., Dekker, S.C., Bouten, W., Bosveld, F.C., Kohsiek, W., Kramer, K., Mohren, G.M.J., 2000. Modeling daily gas exchange of a Douglas-fir forest: comparison of three stomatal conductance models with and without a soil water stress function. Tree Physiol. 20, 115–122.

Whitley, R., Taylor, D., Macinnis-Ng, C., Zeppel, M., Yunusa, I., O'Grady, A., Froend, R., Medlyn, B., Eamus, D., 2013. Developing an empirical model of canopy water flux describing the common response of transpiration to solar radiation and VPD across five contrasting woodlands and forests. Hydrol. Process. 27, 1133–1146, http://dx.doi.org/10.1002/hyp.9280

Wilson, K., Goldstein, A., Falge, E., Aubinet, M., Baldocchi, D., Berbigier, P., Bernhofer, C., Ceulemans, R., Dolman, H., Field, C., Grelle, A., Ibrom, A., Law, B., Kowalski, A., Meyers, T., Moncrieff, J., Monson, R., Oechel, W., Tenhunen, J., Valentini, R., Verma, S., 2002. Energy balance closure at FLUXNET sites. Agric. For. Meteorol. 113, 223–243, http://dx.doi.org/10.1016/S0168-1923(02) 109-0

Wong, S., Cowan, I., Farquhar, G., 1979. Stomatal conductance correlates with photosynthetic capacity. Nature 282, 424–426.

Wright, I.J., Reich, P.B., Cornelissen, J.H.C., Falster, D.S., Groom, P.K., Hikosaka, K., Lee, W., Lusk, C.H., Niinemets, Ü., Oleksyn, J., Osada, N., Poorter, H., Warton, D.I., Westoby, M., 2005. Modulation of leaf economic traits and trait relationships by climate. Global Ecol. Biogeogr. 14, 411–421, http://dx.doi.org/10.1111/j.1466-822x.2005.00172.x

Wullschleger, S.D., 1993. Biochemical limitations to carbon assimilation in C3 plants–a retrospective analysis of the A/Ci curves from 109 species. J. Exp. Bot. 44, 907–920.

Xu, L., Baldocchi, D.D., 2003. Seasonal trends in photosynthetic parameters and stomatal conductance of blue oak (*Quercus douglasii*) under prolonged summer drought and high temperature. Tree Physiol. 23, 865–877.

Zhou, S., Duursma, R.A., Medlyn, B.E., Kelly, J.W.G., Prentice, I.C., 2013. How should we model plant responses to drought? An analysis of stomatal and non-stomatal responses to water stress. Agric. For. Meteorol. 182–183, 204–214, http://dx.doi.org/10.1016/j.agrformet.2013.05.009.